Research Square

Preprints are preliminary reports that have not undergone peer review.
They should not be considered conclusive, used to inform clinical practice,
or referenced by the media as validated information.

A synthetic self-adjuvanted polymeric hapten vaccine enables durable protective immunity after a single immunization

D. Scott Wilson

scott.wilson@jhmi.edu

Johns Hopkins University https://orcid.org/0000-0001-8029-1036

Sandeep Kumar

Johns Hopkins University

Zhuqin Li

Johns Hopkins University

Mengheng Yang

Johns Hopkins University

Sabrina Chen

Johns Hopkins University

Chantelle Terrillion

Johns Hopkins University School of Medicine

Article

Keywords:

Posted Date: November 26th, 2026

DOI: https://doi.org/10.21203/rs.3.rs-11685190/v1

License: This work is licensed under a Creative Commons Attribution 4.0 International License.
Read Full License

Additional Declarations: There is **NO** Competing Interest.

A synthetic self-adjuvanted polymeric hapten vaccine enables durable protective immunity after a single immunization

Sandeep Kumar[1,2], Zhuqin Li[1,2], Mengheng Yang[1,2], Sabrina Chen[1,2], Chantelle Terrillion[3], and D. Scott Wilson[1,2*]

1. Translational Therapeutics and Regenerative Engineering Center, Johns Hopkins University School of Medicine, Baltimore, MD, USA.
2. Department of Biomedical Engineering, Johns Hopkins University School of Medicine, Baltimore, MD, USA.
3. Department of Psychiatry and Behavioral Sciences, Johns Hopkins Hospital, Baltimore, MD, USA.

*Corresponding author: Scott.wilson@jhmi.edu

Abstract: Conventional hapten–carrier protein vaccines against drugs of misuse and other small-molecule targets often generate antibody responses of insufficient magnitude and durability for clinical efficacy. Here we report a synthetic polymeric hapten vaccine that molecularly integrates multivalent antigen display, B cell-intrinsic innate stimulation and carrier-specific T cell help within a single construct. The resulting **p**olymeric **T**LR7/8 self-adjuvanted **f**entanyl **v**accine (pTFV) comprises a carrier protein (CP) linked through a self-immolative linker to a synthetic block copolymer displaying fentanyl haptens and a B cell-activating TLR7/8 agonist. Compared with a conventional monomeric fentanyl vaccine (mFV), pTFV generated a ~7,000-fold higher anti-fentanyl antibody response, increased long-lived antibody-secreting cells and maintained protective antibody titers for at least one year. A single dose of pTFV also provided greater protective immunity than two mFV doses admixed with matched TLR7/8 agonist. These findings demonstrate that integrating multivalent BCR engagement, B cell-intrinsic innate activation, and carrier-specific T cell help within a single construct enables long-lasting protection after a single immunization.

Main: Hapten vaccines have long been pursued as interventions against drugs of misuse and other toxic small-molecule targets. By eliciting target-specific antibodies, these vaccines aim to sequester small molecules in the periphery and prevent them from reaching the location where they exert their harmful biological effects [1,2]. In the context of drugs of misuse, this strategy aims to block drug entry into the brain, thereby providing passive, persistent protection against overdose and drug-induced euphoria[3]. Achieving such protection is particularly challenging because anti-drug vaccines must generate sufficiently high concentrations of pre-existing antibodies to rapidly intercept bolus doses before they reach the brain. Moreover, substance use disorder is a chronic condition with a persistent risk of relapse, requiring long-lived antibody responses that remain protective throughout recovery[4]. Although multidose vaccine regimens can amplify and sustain humoral immunity, reliance on repeated booster immunizations increases treatment burden and creates opportunities for incomplete vaccination, especially in populations with poor healthcare engagement[5]. Indeed, clinical trials of multidose monomeric cocaine and nicotine vaccines failed to generate or sustain antibody responses sufficient for clinical benefit in most participants[6,7]. Thus, effective hapten vaccines must not only generate stronger and more durable antibody responses, but ideally with fewer immunizations.

Durable antibody production is sustained by long-lived antibody-secreting cells (LLASCs), which arise primarily from germinal-center (GC) responses[8]. Within GCs, antigen-specific B cells undergo affinity maturation and selection through interactions with $CD4^+$ T follicular helper (Tfh) cells[9] which provide co-stimulatory signals supporting B cell survival, affinity maturation[10], and differentiation into LLASCs[11,12]. Durable humoral responses are enhanced when antigen-specific B cells receive three signals in close spatial and temporal proximity[13]: multivalent B cell receptor (BCR) engagement, B cell-intrinsic innate activation[14]and cognate $CD4^+$ T cell help[15]. Conventional hapten vaccines attempt to provide these signals by conjugating multiple monomeric haptens to immunogenic CPs and administering the conjugates with admixed adjuvants[16,17,18] (**Fig. S1**). Although hapten-CP linkage couples BCR recognition and internalization to CP-mediated T cell help, adjuvant uptake occurs independently of conjugate internalization and therefore does not ensure innate stimulation of the same antigen-engaged B cell. Hapten–CP modification also creates a trade-off between hapten valency and CP immunogenicity. Although increasing hapten density can enhance multivalent display, covalent CP modification can compromise CP-derived peptide presentation to and recognition by CP-

specific T cells, diminishing T cell responses and expanding regulatory T cells (Tregs)-immune suppressive $CD4^+$ T cells that can dampen vaccine responses[19,20,21,22].Together, these limitations suggest that vaccine architecture, the molecular organization and connectivity of individual components, may critically influence the magnitude, quality, and durability of humoral immunity.

We therefore hypothesized that integrating multivalent BCR engagement, B cell-intrinsic innate activation and CP-mediated T cell help within a single molecular construct would enhance the magnitude and durability of hapten-specific immunity. To test this concept, we engineered water-soluble synthetic copolymers displaying small-molecule haptens together with a TLR7/8 agonist and conjugated them to the FDA-approved carrier protein CRM_{197} through a self-immolative linker[23] (**Fig. 1a,i**). The resulting architecture is designed to couple multivalent hapten recognition and BCR-mediated internalization (**Fig. 1a,ii**) with intracellular release of CRM_{197} for efficient processing and presentation to carrier-specific T cells (**Fig. 1a,iii**), while the polymer-bound TLR7/8 agonist provides innate stimulation to the antigen-engaged B cell (**Fig. 1a,iv**). Thus, three complementary signals for durable humoral immunity are molecularly integrated within a single vaccine construct (**Fig. 1a,v**).

Here we apply this strategy to fentanyl, an urgent clinical target, and a stringent test of antibody-mediated protection. Using pTFV, we systematically evaluated how synthetic polymer design influences vaccine performance by varying TLR7/8 integration, the spatial organization of fentanyl haptens within block versus random copolymers, and controlled CP release. These studies show that integrating these signals within a single construct substantially increases vaccine potency and durability, enabling long-lasting protective immunity after a single immunization. Substitution of fentanyl with the chemically distinct hapten 4-hydroxy-3-nitrophenylacetic acid (NP) further demonstrates the adaptability of the architecture. Together, these findings establish molecular integration of antigen display, innate stimulation, and T-cell help as an engineering strategy for generating durable protective immunity against small-molecule targets.

Results: Polymer engineering enables an integrated, multifunctional hapten vaccine architecture. To create a synthetic polymeric fentanyl vaccine that integrates multivalent hapten

display, TLR7/8 stimulation, and releasable carrier-mediated T cell help within a single construct, we synthesized pTFV using a modular three-step strategy. First, we prepared p(TLR-*b*-Fent), a water-soluble block copolymer containing spatially distinct TLR7/8 agonist- and fentanyl-bearing segments (**Fig. 1b**). We chose to target B cell TLR7/8 because TLR7 and TLR7/8 signaling are potent amplifiers of B cell development and antibody-secreting cell differentiation in rodents[24] and humans[25], respectively. Although murine cells are insensitive to small-molecule TLR8 agonist[26], we incorporated dual TLR7/8 activity for greater relevance to human immunity and future clinical translation. The first block, p(TLR) **4**, was prepared by reversible addition–fragmentation chain-transfer (RAFT) polymerization using a difunctional azide- and fentanyl-terminated RAFT agent **1**, a methacrylamide-functionalized TLR7/8 agonist **2** (mTLR), and a biologically inert comonomer **3**. The resulting p(TLR) macro-chain-transfer agent (**4**) was subsequently chain-extended with a second RAFT polymerization utilizing a methacrylamide-functionalized fentanyl analog **5** (mFent) and the same inert comonomer to generate p(TLR-*b*-Fent) **6**. The resulting polymer had an average molecular weight of ~44 kDa and contained 3.5 and 3.0 mol% mTLR and mFent, respectively (**Table S1**). To maximize innate and BCR stimulation, the mTLR and mFent content of each block was set to maximize agonist loading while maintaining polymer water-solubility. The lengths of both polymer blocks were similarly maximized while controlling polymer polydispersity (data not shown).

To attach p(TLR-*b*-Fent) to CRM_{197} via a reversable linkage, we synthesized a bifunctional poly (ethylene glycol) linker (**10**) terminated with an amine-reactive N-hydroxysuccinimide carbonate and an azide-reactive dibenzocyclooctyne (**Fig. S2a**). Conjugation of the linker to CRM_{197} generates a reduction-sensitive, self-immolative linkage that is relatively stable, but is designed to release unmodified CRM_{197} upon internalization[27] (**Fig. 1c, d, S2b**). p(TLR-*b*-Fent) was subsequently attached to the modified CRM_{197} through a copper-free, strain promoted click reaction between the p(TLR-*b*-Fent)'s terminal azide and our linker's dibenzocyclooctyne, yielding pTFV (**Fig. 1d, Fig. S2d).** MALDI-TOF mass spectrometry and spectrophotometric analyses indicated that an average of ~7 DBCO bearing linkers were conjugated to each CRM_{197} molecule (**Fig. S2c**), corresponding to an mTLR: CRM_{197} mass ratio of ~1:1. Polymer vaccine lacking the incorporated TLR7/8 agonist (pFV) were synthesized and characterized (**Scheme S15**, **Fig. S2e**) using analogous procedures.

Conventional monomeric hapten–carrier vaccines (mFV) were synthesized using a previously reported procedure[24,28]. Prior fentanyl-CRM_{197} vaccines have employed hapten densities ranging from 2[29] to 15[30] fentanyl haptens per CRM_{197}. MALDI-TOF analysis revealed that we achieved an average loading of ~9.5 fentanyl haptens per CRM_{197} (**Fig. S2f-i**), within the range associated with optimal immunogenicity for CRM_{197}-based opioid vaccines[31].

A polymeric vaccine architecture that molecularly integrates antigen recognition, innate stimulation, and T cell help enhances hapten vaccine efficacy. To determine whether the integrated polymer architecture of pTFV contributes to its enhanced efficacy, we compared pTFV to formulations in which innate stimulation or CP-mediated T cell help was uncoupled from the polymeric scaffold. Mice (n = 6/group) were vaccinated with saline, a polymeric fentanyl vaccine lacking polymer-incorporated TLR7/8 agonist (pFV) admixed with soluble mTLR (pFV + mTLR); or a physical mixture of (p(TLR-*b*-Fent) + CRM_{197}) (**Fig. 1e**).

At week 9, mice vaccinated with pTFV experienced an approximately 100-fold greater anti-fentanyl IgG titer (**Fig. 1f, S3a-f**) and a superior antibody avidity index than either control formulation (**Fig. 1g, S3g**). These improvements translated into functional protection, as only pTFV significantly reduced fentanyl-induced analgesia following intraperitoneal (i.p.) fentanyl challenge, as measured by percent maximal possible effect (%MPE) (**Fig. 1h**). Together, these results demonstrate that molecular integration of innate stimulation and CRM_{197}-mediated T cell help are critical to the magnitude, quality, and protective efficacy of the pTFV response.

Spatial control of polymeric hapten display enhances vaccine efficacy. We next asked whether the spatial organization of hapten within the polymer further influences vaccine efficacy. We compared pTFV, synthesized from block copolymers (p(TLR-*b*-Fent)) to (pTFV-R), a polymeric TLR7/8-self-adjuvanted fentanyl vaccine formulation synthesized from random copolymers (p(TLR-*co*-Fent)) (**Scheme S16**). The key structural distinction is that in pTFV, the fentanyl monomers are localized within the polymer block distal to CRM_{197}, reducing potential steric interference from CRM_{197} and polymeric scaffold that could block BCR engagement. Mice were vaccinated on days 0 and 21 with saline, or pTFV, or pTFV-R (**Fig. 1i**).

Our block polymer vaccine, pTFV, elicited higher anti-fentanyl IgG titers than pTFV-R over the course of the experiment (**Fig. 1j, S4a-g**) and generated antibodies with significantly greater

avidity (**Fig. 1k, S4h**). Importantly, following fentanyl challenge, only pTFV-vaccinated mice exhibited a significant reduction in fentanyl-induced analgesia (**Fig. 1l**). These findings demonstrate that the spatial organization of hapten within the synthetic polymer scaffold is an important determinant of vaccine efficacy.

Self-immolative CRM_{197} release enhances T cell help, GC and antibody responses. Previous studies have shown that covalent CP modification can diminish CP immunogenicity by disturbing CP processing into peptides and the presentation and recognition of CP-derived peptides to and by CP-specific T cells[19,32]. Thus, we incorporated a self-immolative linker into pTFV to release unmodified CP following internalization. To directly evaluate CP-specific T cell responses, we synthesized pTFV using ovalbumin (OVA) as the CP ($pTFV_{OVA}$), together with a composition-matched vaccine containing a non-self-immolative linker ($pTFV_{OVA}$-NS) (**Scheme S17**) and a corresponding monomeric vaccine admixed with mTLR (mFV_{OVA}+ mTLR) (**Fig. S5a-c**). To assess CP-specific T cell responses, mice received adoptively transferred OVA-specific $CD4^+$ T cells (OTII T cells) one day before vaccination. The mice were then immunized and OVA-specific $CD4^+$ T cell responses, GC B cell development, and antibody responses were evaluated as shown in Figure 2a.

$pTFV_{OVA}$ generated the strongest OVA-specific $CD4^+$ T cell response among the vaccine formulations (**Figs. 2b-g, S6-9**). Only $pTFV_{OVA}$ significantly increased the abundance of draining lymph node (dLN) OTII $CD4^+$ T cells relative to saline controls (**Figs. 2b, c**), a result consistent with enhanced antigen-recognition by OTII T cells[33]. This response was accompanied by substantially greater Tfh differentiation, as only $pTFV_{OVA}$ generated a significant increase in the frequency of OTII Tfh cells in the dLNs (**Fig. 2d, S6**). Additionally, following *ex vivo* OVA restimulation, dLN cell populations from mice immunized with $pTFV_{OVA}$ contained significantly greater frequencies of cytokine-producing OTII $CD4^+$ T cells, including 75-fold more $TNF\alpha^+$, 12-fold more $IFN\gamma^+$, and 1.8-fold more multifunctional $TNF\alpha^+IFN\gamma^+$ $CD4^+$ T cells than mFV_{OVA} + mTLR (**Figs. 2e-g, S7-8**). In parallel, $pTFV_{OVA}$ sharply reduced the frequency of OVA-specific Tregs relative to the other vaccines (**Figs. 2h, I, S9**), indicating that self-immolative carrier release favored a helper-associated rather than regulatory OVA-specific T cell response.

The enhanced carrier-specific T cell response was accompanied by greater GC activity and humoral immunity. $pTFV_{OVA}$ generated significantly higher GC B cell frequencies (**Figs. 2j, k, S10**) and elicited the strongest anti-fentanyl antibody response among the vaccine formulations (**Fig. 2l**). Similar results were observed in the spleen (**Fig. S11**). In conclusion, these findings provide functional evidence that self-immolative CP release enhances the cellular machinery that drives humoral immunity and is a critical functional element of the pTFV architecture.

Polymeric vaccines provide durable, dose-sparing protection that exceeds monomeric vaccines. To benchmark the long-term efficacy of pTFV, mice were vaccinated with saline, pTFV (4 or 18 μg), or a monomeric fentanyl vaccine (18 μg) formulated with the identical TLR7/8 agonist (mFV + mTLR) according to the schedule shown in Figure 3a. Anti-fentanyl IgG responses were monitored for 52 weeks, followed by fentanyl challenge and quantification of bone marrow-resident LLASCs.

Despite being administered at a 4.5-fold lower dose, 4 μg of pTFV elicited higher anti-fentanyl IgG titers than 18 μg of mFV + mTLR at every measured time point, including both the peak (week 9) and durable (week 52) responses (**Fig. 3b**). Moreover, antibody titers elicited by pTFV at both doses remained stable throughout the 52-week study, whereas those induced by mFV + mTLR declined over time (**Fig. 3c, S12a-m**). pTFV also generated antibodies with significantly greater avidity (**Fig. 3d, S12n**), increased the frequency of fentanyl-specific LLASCs in the bone marrow (**Fig. 3e, f**), and provided superior protection against fentanyl challenge one year after vaccination (**Fig. 3g**). The breadth of this response extended to carfentanil, an analogue 100-fold more potent than fentanyl[34], with pTFV eliciting anti-carfentanil IgG responses greater than those induced by mFV + mTLR despite the 4.5-fold lower vaccine dose (**Fig. 3h, S12o**). Importantly, the efficacy advantage of the polymeric vaccine over its monomeric counterpart was maintained when fentanyl was replaced with NP (**Scheme S18, Fig. S13**), demonstrating that the benefits of our polymeric architecture extend beyond a single hapten.

We next asked whether the advantages of pTFV extended to comparison with alum, the adjuvant used in clinical trials of conventional monomeric cocaine and nicotine vaccines and the most widely used adjuvant in licensed human vaccines [6,27,28]. Mice were vaccinated with pTFV (4 or 18 μg) or 18 μg of mFV formulated with alum and evaluated over 30 weeks (**Fig. 3i).** Both the

high and low doses of pTFV generated substantially higher anti-fentanyl IgG titers than the high dose of mFV + alum beginning two weeks after vaccination and maintained this advantage throughout the study (**Fig. 3j, S14a-g**). This superior antibody response resulted in a significant decrease in fentanyl-mediated analgesia (**Fig. 3k**). pTFV also generated greater anti-carfentanil antibody responses than mFV + alum while requiring substantially lower antigen doses (**Fig. 3l, S14h**). In concert, these findings demonstrate that our polymeric vaccine architecture generates durable, dose-sparing humoral immunity that exceeds monomeric vaccines across multiple haptens and mFV formulated with either matched TLR7/8 adjuvant or alum.

A Single-dose of pTFV outperforms two-doses of monomeric fentanyl vaccine. Although conventional mFVs have employed multidose regimens to achieve protection in rodents, repeated immunization represents an important practical limitation for anti-drug vaccines. Completion of multidose vaccination regimens can be poor among people with opioid use disorder, with some studies reporting completion rates of only 14–41% [35]. More broadly, vaccine acceptance can decline with successive booster doses[36,37], while each additional immunization increases exposure to vaccine-associated reactogenicity. Given the advantages of single-does vaccine regimens, we compared the immunogenicity, durability, and protective efficacy of one dose of pTFV with those of a two-dose regimen of mFV + mTLR (**Fig. 4a**).

A single immunization with pTFV elicited a markedly stronger and more durable anti-fentanyl antibody response than two doses of mFV + mTLR (**Fig. 4b, S15a-k**) and generated antibodies with significantly greater avidity (**Fig. 4c, S15l**). This enhanced humoral response was accompanied by an approximately 25-fold increase in fentanyl-specific LLASC in the bone marrow (**Fig. 4e, f**). Importantly, these immunological advantages were translated into superior functional protection. Following fentanyl challenge, mice receiving a single dose of pTFV exhibited significantly reduced fentanyl-induced analgesia (**Fig. 4d**). These findings demonstrate that the synthetic polymeric vaccine architecture can outperform a conventional monomeric vaccine despite requiring half as many administrations.

Finally, we assessed whether vaccine-induced antibodies retain specificity in the presence of clinically relevant μ-opioid receptor-binding molecules. A competitive ELISA performed with naloxone, an opioid antagonist that is used for reversing overdose, showed no effect of naloxone

competition on the binding of pTFV-induced antibodies to fentanyl, indicating preserved specificity for the target structural hapten (**Fig 4g**).

Single dose of our polymeric vaccine provides superior durable protection across conventional adjuvant benchmarks. We next benchmarked the single-dose efficacy of pTFV against dose-matched monomeric fentanyl vaccines (mFV) formulated with CpG, poly(I:C), alum, or alum + CpG-adjuvants that have previously demonstrated efficacy in multidose monomeric fentanyl vaccine regimens[38,39]. Mice were immunized once and monitored for 30 weeks according to Figure 5a.

pTFV elicited significantly higher anti-fentanyl IgG titers than the monomeric formulations as early as week 2 and at every time point after week 5 (**Fig. 5b**). By week 30, anti-fentanyl IgG titers were ~40-fold greater than those elicited by mFV + alum + CpG, the most immunogenic monomeric formulation (**Fig. 5c, S16a-m**). Consistent with the durability of this response, pTFV was the only vaccine to significantly increase fentanyl-specific LLASCs in the bone marrow at week 30 (**Fig. 5d, e**). These immunological differences translated into functional protection as only pTFV significantly reduced fentanyl-induced analgesia 30 weeks after a single immunization (**Fig. 5f**). In sum, these observations demonstrate that the integrated synthetic polymeric architecture of pTFV generates substantially greater, more durable, and more protective single-dose immunity than monomeric fentanyl vaccines formulated with established adjuvants[40].

Discussion: In sum, these findings establish a synthetic polymeric hapten vaccine strategy in which polymer engineering controls antigen valency, molecular organization, innate stimulation and carrier-mediated T cell help. By transferring multivalent hapten display from the CP to a synthetic polymer scaffold, this architecture decouples antigen valency from extensive carrier modification, enabling independent control over BCR engagement and CP function. Vaccine performance depended not simply on the presence of individual components, but on their molecular organization. Rearranging closely matched amounts of fentanyl, TLR7/8 agonist from a block to a random polymer architecture altered antibody magnitude, avidity and protection. Similarly, uncoupling TLR7/8 stimulation from the antigenic construct reduced immunogenicity and efficacy, whereas preventing self-immolative carrier release diminished multifunctional CP-

specific $CD4^+$ T cell responses, germinal-center B cell responses and antibody production. Collectively, these experiments demonstrate that the enhanced efficacy of pTFV arises from molecular integration of complementary immune signals rather than simply from their inclusion within the same formulation.

Previous studies have utilized synthetic polymers to display multivalent B cell haptens to demonstrate that polymer hapten conjugate vaccines can improve B cell responses[41,42]. However, these platforms relied on separately administered innate adjuvants, and protective efficacy was not established. Our results show that extending a polymeric hapten construct to include molecularly integrated innate stimulation is more effective than simply combining a polymeric hapten conjugate vaccine with an admixed adjuvant. Our architecture coordinates BCR engagement, B cell-intrinsic innate activation and carrier protein release within a single molecular construct, thereby extending polymeric haptens from multivalent antigen scaffolds to multifunctional architectures capable of durable functional protection.

These architectural advantages translated into exceptional potency, durability, and vaccination efficiency. pTFV generated high-magnitude, high-avidity antibody responses, increased fentanyl-specific long-lived antibody-secreting cells, maintained protective immunity for at least one year, and produced superior responses at substantially lower doses than the corresponding mFV. Moreover, a single pTFV immunization generated stronger and more durable protection than two doses of the corresponding monomeric vaccine and exceeded single-dose monomeric vaccines formulated with established adjuvants. The combination of tunable molecular organization, multifunctional signal integration, exceptional durability, single-dose efficacy, and hapten modularity position synthetic polymer engineering as a powerful framework for generating protective immunity to toxic small molecules.

Methods. Cell culture-grade media, fetal bovine serum, antibiotics, flow cytometry reagents, antibodies for flow cytometry, and chemicals for synthesis were procured from various sources detailed in supplementary data table 2. The endotoxin levels of all vaccine formulations were determined using ToxinSensor™ chromogenic LAL endotoxin assay kit (Genscript). A detailed experimental synthesis protocols and characterization of all polymers, monomer conjugates and intermediates are provided in Supplementary information.

Vaccine preparation and characterization.

Details of vaccine preparation and characterization are provided in the supplementary information. Briefly, DBCO-labeled carrier protein (OVA, and CRM_{197}) conjugates (CP-DBCO) were prepared by reacting the proteins with a 20-fold molar excess of self immolative linker (**11**). After purification via size exclusion chromatography, CP-DBCO was reacted with a 10-fold weight excess of azido-terminated fentanyl-decorated polymer p(TLR-*b*-Fent) or p(Fent), or p(TLR-*co*-Fent) or NP-decorated polymer p(TLR-*b*-NP). The mixture was stirred for 5 hours at r.t. and purified via fast protein liquid chromatography (FPLC) using 1xPBS as mobile phase. Fractions were collected and analyzed by gel electrophoresis. Fractions containing carrier protein-polymer conjugates were pooled and concentrated using an Amicon ® Ultra 4 mL, 10 kDa filtration device. Protein concentration was determined by gel electrophoresis, and mTLR concentration was measured via mTLR-specific absorbance at 327 nm (Nanodrop, Thermo). Polymeric conjugate vaccines were characterized by via size exclusion chromatography-high-performance liquid chromatography (SEC-HPLC) using 1x PBS as mobile phase.

Monomeric BSA/OVA/CRM-fentanyl conjugate vaccine (mFV).

All carrier proteins, including BSA, OVA, and CRM_{197}, were prepared as stock solutions at ~10 mg/mL in 1X PBS (pH 7.4). Stock solutions were then mixed with a 20-fold molar excess of the respective hapten-NHS ester (listed in detail in supplementary information). After 3 h, the final conjugates were purified via Zeba spin desalting columns with a 7 kDa cut-off limit (Thermo Fisher). Protein concentration was determined by gel electrophoresis, and the hapten density was determined by MALDI-TOF-MS.

Immunization

The specific details for each immunization study are provided in the supplementary information. In general, C57BL/6 mice were vaccinated via subcutaneous (s.c) injection into the four footpads on days 0 and 21. Blood samples were collected from mice at various time points using facial vein sampling. The serum was then separated from the blood cells by centrifugation at 4000x G for 15 minutes and stored at −20 ºC. At the termination of some experiments, mice were challenged with fentanyl and bone marrow cells were collected for ELISpot analysis.

Enzyme Linked Immunosorbent Assay (ELISA).

End-point antibody titers were determined by standard ELISA. Briefly, 96-well plates were coated overnight at 4 °C with 10 μg/mL hapten–BSA conjugate or CRM_{197}. Plates were washed and blocked for 2 h at r.t. Serum samples were serially diluted in blocking buffer, transferred to the plates, and incubated for 2 h at r.t. After washing, horseradish peroxidase (HRP)-conjugated secondary antibody (anti-mouse-IgG-HRP, Southern Biotech, USA) was added and incubated for 1h at r.t. Plates were developed using 3,3′,5,5′-tetramethylbenzidine (TMB) substrate, and the reaction was stopped with 1 M H_2SO_4. Absorbance was measured at 450 nm, and end-point titers were calculated using GraphPad Prism 10.

Antibody avidity was determined by chaotropic ELISA. Following serum incubation, plates were treated with increasing concentrations of guanidine hydrochloride in PBS for 1 h at r.t. before addition of the HRP-conjugated secondary antibody. The avidity index was defined as the guanidine hydrochloride concentration (M) at which the normalized OD_{450} reached 0.5. Values were determined by smoothing fit spline interpolation with 500 segments in GraphPad Prism 10.

Cross-reactivity of anti-serum containing anti-fentanyl antibodies to naloxone was evaluated by competitive inhibition ELISA where serum samples (1:1000x dil) and naloxone (0-200 ng/mL) were premixed with various concentrations and added to BSA-mFent coated ELISA plates. The absorbance at 450 nm was measured before and after naloxone treatment to assess the response.

$CD4^+$ T cell immune responses (Flow cytometry)

Single cells suspensions from spleen and dLN were obtained via mechanical disruption of the organs and a subset of these cells were cultured in complete media or OVA-spiked (200 μg/ml) complete media for 3 h before brefeldin a was added and the cells cultured for another 5 h.

OVA-restimulated cells and single cells suspensions from spleen and dLN were stained with LIVE/DEAD™ Fixable Near-IR Stain (ThermoFisher) for 30 min at r.t. and washed with FACS buffer (PBS + 2% FBS). Cells were then incubated with Fc block (TruStain FcX™) for 30 min at 4 °C. The OVA-restimulated cells were then stained for 45 min with antibodies identifying T cell subsets (CD3, CD4, CD8) prepared in FACS buffer. Unstimulated cells were incubated with

antibody cocktails to determine GC B cells (CD19, B220, GL7, CD95), T follicular helper cells (CD3, CD4, CD8, CD44, CXCR5, PD-1, CD45.1), and Tregs (CD3, CD4, CD8, CD45.1, CD25). Stained cells were washed 2x with PBS and fixed for 45 min at r.t. in eBioscience™ Foxp3 / Transcription Factor Fixation/Permeabilization Concentrate and Diluent (1:3 v/v) buffer. Restimulated cells and the cells stained with Tfh cell- and Treg-identifying antibodies were washed with FACS buffer and permeabilized using 1x Perm buffer for 5 min. Intracellular staining (Bcl-6 for Tfh panel; FOXP3 for Treg panel; and TNFα, IFNγ for restimulated Tcells panel) was carried out in permeabilization buffer at 4 °C for 1 h. After washing all cells with FACS buffer twice, cell samples were resuspended in FACS buffer and assessed via flow cytometry (Attune NxT Flow Cytometer, Thermo Fisher). The data was analyzed using FlowJo version 10.10.0 (Becton Dickinson & Company, BD). Antibodies and reagents used for flow cytometry are listed in Table S2.

ELISpot assay.

LLASCs were identified using ELISpot Flex: Mouse IgG (ALP) kit (Cat# 3825-2A, MABTECH, Sweden) in 96-well BSA fentanyl-coated hydrophobic filter plates (Millipore, USA) as per manufacturer's guidelines. The ELISpot assay was carried out with dilutions of bone marrow cells (100k, 250k, 500k and $1x10^6$ cell per well) and spots were generated using BCIP/NBT as a substrate and counted by ImmunoSpot® Reader and ImmunoSpot 7.0.38.7 software (Cellular Technology Limited, Cleveland, USA). Data is presented as Fentanyl specific antigen secreting cells (ASCs) spots per 10^6 cells in mouse bone marrow.

Fentanyl challenge study (hot plate assay).

Vaccine protective efficacy against fentanyl was evaluated using hot-plate antinociception assay. For the hot-plate assay, mice were placed on a surface maintained at 55 ± 0.2 °C, and the latency to the first nociceptive response, defined as hind-paw licking, paw withdrawal or shaking, or jumping, was recorded. A 45-sec cutoff was used to prevent tissue injury. Baseline response latencies were measured before the fentanyl challenge. Following intraperitoneal (i.p) fentanyl administration (0.3 mg/kg), nociceptive testing was repeated at 30 minutes. Antinociception was expressed as the percentage of the maximum possible effect (%MPE), calculated as:

%MPE = [(test latency − baseline latency)/(45 − baseline latency)] × 100.

Statistical analysis.

Data are presented as the mean ± s.d. and analyzed using GraphPad Prism 10. Unpaired t-test as Mann-Whitney test with compared ranks was utilized to compare the difference between two groups and ordinary one-way ANOVA with Tukey's multiple comparisons test was performed to compare the difference between more than two groups. Horizontal lines identify the groups being compared, and *P* values are shown above the corresponding lines.

Data availability

All data supporting this study are available in the manuscript and its supplementary information. Source data is provided with this paper, and additional data will be provided on request to the corresponding author.

Acknowledgements

This work was supported by NIH National Institute of Biomedical Imaging and Bioengineering (R21EB031347), NIH National Institute on Drug Abuse (R21DA054740), NIH National Institute of Allergy and Infectious Diseases (DP2AI164306), Johns Hopkins University Discovery Award, and PhRMA Foundation Faculty Starter Grant. Sabrina Chen was supported by NSF Graduate Research Fellowship Program (GRFP) (DGE2139757). Dr. Shridhar (Shri) Bhat assisted us in NMR analysis, and we are grateful to NIH for supporting the JHU-SOM NMR facility through award number S10OD034217. We also thank Dr. Stephane Lajoie's lab for providing OTII mice breeding pair. Additionally, we acknowledge the support of Johns Hopkins University School of Medicine animal facility, SKCCC Immune Monitoring Core, behavioral core.

Author contributions

D.S.W conceived the idea and supervised the studies. S.K. conducted polymer synthesis, including characterization, vaccine synthesis, vaccination experiments, flow cytometry analysis,

ELISPOT assays, and data analysis. S.K. and Z.L. performed ELISA assays. S.K., M.Y., Z.L. and C.T. performed the hot plate assays. S.K., M.Y., V.H. and J.Z. performed the chemical synthesis of monomers. S.K and D.S.W wrote the manuscript and with input from all the co-authors.

References.

1. Hosztafi, S. *et al.* Opioid-Based Haptens: Development of Immunotherapy. *Int. J. Mol. Sci.* **25**, 7781 (2024).

2. Bremer, P. T., Janda, K. D. & Barker, E. L. Conjugate Vaccine Immunotherapy for Substance Use Disorder. *Pharmacol. Rev.* **69**, 298–315 (2017).

3. Hamid, F. A., Siram, K., Burkhart, D., Evans, J. T. & Pravetoni, M. Mechanistic insights into the cellular and molecular mechanisms of an anti-opioid vaccine formulated with a novel Toll-Like receptor (TLR) 7/8 agonist. *J. Pharmacol. Exp. Ther.* **389**, 480 (2024).

4. Knopf, A. Consider new options for treating OUD in designing trials. *Alcohol. Drug Abus. Wkly.* **35**, 5–5 (2023).

5. Ramasamy, P. *et al.* The outcome of a rapid hepatitis B vaccination programme in a methadone treatment clinic. *Addiction* **105**, 329–334 (2010).

6. Kosten, T. R. *et al.* Vaccine for cocaine dependence: A randomized double-blind placebo-controlled efficacy trial. *Drug Alcohol Depend.* **140**, 42–47 (2014).

7. Truong, T. T. & Kosten, T. R. Current status of vaccines for substance use disorders: A brief review of human studies. *J. Neurol. Sci.* **434**, 120098 (2022).

8. Silva, N. S. D. & Klein, U. Dynamics of B cells in germinal centres. *Nat. Rev. Immunol.* **15**, 137–148 (2015).

9. Schrock, D. C. *et al.* Pivotal role for αV integrins in sustained Tfh support of the germinal center response for long-lived plasma cell generation. *Proc. Natl. Acad. Sci.* **116**, 4462–4470 (2019).

10. Pagan, J. D., Vlamakis, H., Gaca, A., Xavier, R. J. & Anthony, R. M. Modulating T Follicular Cells In Vivo Enhances Antigen-Specific Humoral Immunity. *J. Immunol.* **206**, 2583–2595 (2021).

11. Robinson, M. J. *et al.* Long-lived plasma cells accumulate in the bone marrow at a constant rate from early in an immune response. *Sci. Immunol.* **7**, eabm8389 (2022).

12. Shlomchik, M. J. & Weisel, F. Germinal center selection and the development of memory B and plasma cells. *Immunol. Rev.* **247**, 52–63 (2012).

13. Fillatreau, S. & Manz, R. A. Tolls for B cells. *Eur. J. Immunol.* **36**, 798–801 (2006).

14. Browne, E. P. Regulation of B-cell responses by Toll-like receptors. *Immunology* **136**, 370–379 (2012).

15. Ferapontov, A. *et al.* Antigen footprint governs activation of the B cell receptor. *Nat. Commun.* **14**, 976 (2023).

16. Natori, Y. *et al.* A chemically contiguous hapten approach for a heroin–fentanyl vaccine. *Beilstein J. Org. Chem.* **15**, 1020–1031 (2019).

17. Crouse, B. *et al.* A TLR7/8 agonist increases efficacy of anti-fentanyl vaccines in rodent and porcine models. *npj Vaccines* **8**, 107 (2023).

18. Hwang, C. S. *et al.* Improved Admixture Vaccine of Fentanyl and Heroin Hapten Immunoconjugates: Antinociceptive Evaluation of Fentanyl-Contaminated Heroin. *ACS Omega* **3**, 11537–11543 (2018).

19. Singh, K. V., Khanna, P., Suri, C. R. & Garg, M. L. Structural and Immunogenic Effects of Multiple Hapten Loading on Carrier Protein. *J. AOAC Int.* **93**, 59–65 (2010).

20. Stepkowski, S. *et al.* The Major Role of T Regulatory Cells in the Efficiency of Vaccination in General and Immunocompromised Populations: A Review. *Vaccines* **12**, 992 (2024).

21. Gefen, T. *et al.* The effect of haptens on protein-carrier immunogenicity. *Immunology* **144**, 116–126 (2015).

22. Kobayashi, K. *et al.* Reduced Immunogenicity of β-Lactoglobulin by Conjugation with Carboxymethyl Dextran Differing in Molecular Weight. *J. Agric. Food Chem.* **49**, 823–831 (2001).

23. Malito, E. *et al.* Structural basis for lack of toxicity of the diphtheria toxin mutant CRM197. *Proc. Natl. Acad. Sci.* **109**, 5229–5234 (2012).

24. Clingan, J. M. & Matloubian, M. B Cell–Intrinsic TLR7 Signaling Is Required for Optimal B Cell Responses during Chronic Viral Infection. *J. Immunol.* **191**, 810–818 (2013).

25. Auladell, M. *et al.* Distinguishing naive- from memory-derived human B cells during acute responses. *Clin. Transl. Immunol.* **8**, e01090 (2019).

26. Hemmi, H. *et al.* Small anti-viral compounds activate immune cells via the TLR7 MyD88–dependent signaling pathway. *Nat. Immunol.* **3**, 196–200 (2002).

27. Wilson, D. S. *et al.* Synthetically glycosylated antigens induce antigen-specific tolerance and prevent the onset of diabetes. *Nat. Biomed. Eng.* **3**, 817–829 (2019).

28. Robinson, C. *et al.* Therapeutic and Prophylactic Vaccines to Counteract Fentanyl Use Disorders and Toxicity. *J. Med. Chem.* **63**, 14647–14667 (2020).

29. Stone, A. E. *et al.* Fentanyl conjugate vaccine by injected or mucosal delivery with dmLT or LTA1 adjuvants implicates IgA in protection from drug challenge. *npj Vaccines* **6**, 69 (2021).

30. Baehr, C. *et al.* Bivalent Hapten Display Strategies for Conjugate Vaccines Targeting Opioid Mixtures Containing Fentanyl. *Bioconjugate Chem.* **36**, 676–687 (2025).

31. Jalah, R. *et al.* Efficacy, but Not Antibody Titer or Affinity, of a Heroin Hapten Conjugate Vaccine Correlates with Increasing Hapten Densities on Tetanus Toxoid, but Not on CRM197 Carriers. *Bioconjugate Chem.* **26**, 1041–1053 (2015).

32. Gefen, T. *et al.* The effect of haptens on protein-carrier immunogenicity. *Immunology* **144**, 116–126 (2015).

33. Tatsumi, N., Codrington, A. L., El-Fenej, J., Phondge, V. & Kumamoto, Y. Effective CD4 T cell priming requires repertoire scanning by CD301b+ migratory cDC2 cells upon lymph node entry. *Sci. Immunol.* **6**, eabg0336–eabg0336 (2021).

34. Jalal, H. & Burke, D. S. Carfentanil and the rise and fall of overdose deaths in the United States. *Addiction* **116**, 1593–1599 (2021).

35. Nyamathi, A., Sinha, K., Greengold, B., Cohen, A. & Marfisee, M. Predictors of HAV/HBV vaccination completion among methadone maintenance clients. *Res. Nurs. Heal.* **33**, 120–132 (2010).

36. Batra, K., Sharma, M., Dai, C.-L. & Khubchandani, J. COVID-19 Booster Vaccination Hesitancy in the United States: A Multi-Theory-Model (MTM)-Based National Assessment. *Vaccines* **10**, 758 (2022).

37. Motta, M. The Correlates & Public Health Consequences of Prospective Vaccine Hesitancy among Individuals Who Received COVID-19 Vaccine Boosters in the U.S. *Vaccines* **10**, 1791 (2022).

38. Blake, S. *et al.* Developing Translational Vaccines against Heroin and Fentanyl through Investigation of Adjuvants and Stability. *Mol. Pharm.* **18**, 228–235 (2021).

39. Bremer, P. T. & Janda, K. D. Investigating the Effects of a Hydrolytically Stable Hapten and a Th1 Adjuvant on Heroin Vaccine Performance. *J. Med. Chem.* **55**, 10776–10780 (2012).

40. Powers, N. *et al.* Self-Adjuvanting TLR7/8 Agonist and Fentanyl Hapten Co-Conjugate Achieves Enhanced Protection against Fentanyl Challenge. *Bioconjugate Chem.* **34**, 1811–1821 (2023).

41. Lipinski, T., Kitov, P. I., Szpacenko, A., Paszkiewicz, E. & Bundle, D. R. Synthesis and Immunogenicity of a Glycopolymer Conjugate. *Bioconjugate Chem.* **22**, 274–281 (2011).

42. Bennett, N. R. *et al.* Modular Polymer Antigens to Optimize Immunity. *Biomacromolecules* **20**, 4370–4379 (2019).

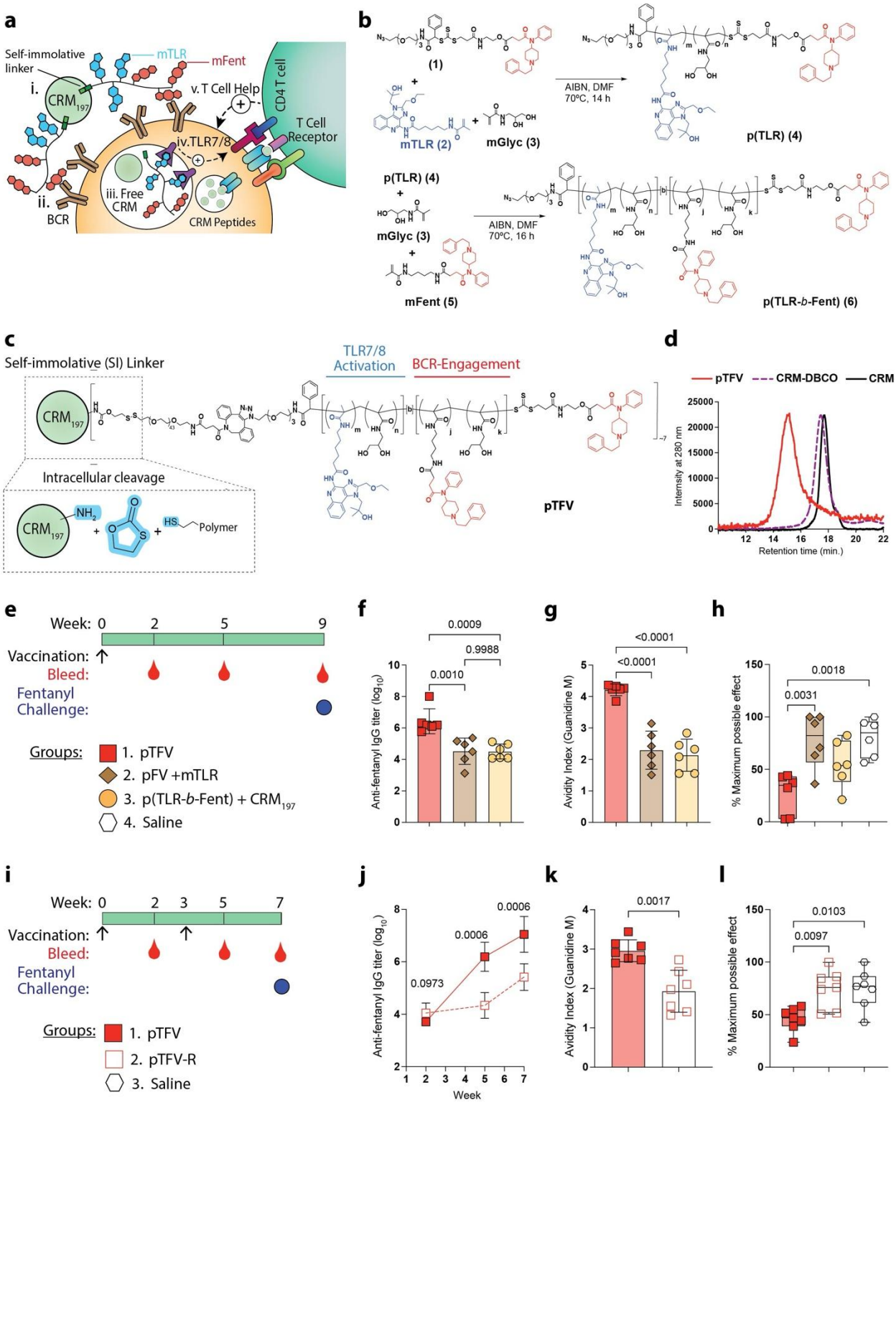
a
Self-immolative linker
mTLR
mFent
i.
CRM197
v. T Cell Help
CD4 T cell
T Cell Receptor
iv.TLR7/8
iii. Free CRM
ii.
BCR
CRM Peptides
b
(1)
mTLR (2)
mGlyc (3)
AIBN, DMF
70°C, 14 h
p(TLR) (4)
mFent (5)
AIBN, DMF
70°C, 16 h
p(TLR-b-Fent) (6)
c
Self-immolative (SI) Linker
TLR7/8 Activation
BCR-Engagement
Intracellular cleavage
Polymer
pTFV
d
pTFV
CRM-DBCO
CRM
Intensity at 280 nm
Retention time (min.)
e
Week: 0 2 5 9
Vaccination:
Bleed:
Fentanyl Challenge:
Groups:
1. pTFV
2. pFV +mTLR
3. p(TLR-b-Fent) + CRM197
4. Saline
f
Anti-fentanyl IgG titer (log10)
0.0009
0.9988
0.0010
g
Avidity Index (Guanidine M)
<0.0001
<0.0001
h
% Maximum possible effect
0.0018
0.0031
i
Week: 0 2 3 5 7
Vaccination:
Bleed:
Fentanyl Challenge:
Groups:
1. pTFV
2. pTFV-R
3. Saline
j
Anti-fentanyl IgG titer (log10)
0.0006
0.0006
0.0973
Week
k
Avidity Index (Guanidine M)
0.0017
l
% Maximum possible effect
0.0103
0.0097

Figure 1. A block polymer vaccine architecture integrating BCR engagement, innate activation, and T cell help enhances anti-fentanyl immunity. (**a**) (i.) Schematic of the polymeric conjugate vaccine platform designed to coordinate (ii.) multivalent B-cell receptor (BCR) engagement, (iii.) release of unmodified carrier protein, (iv.) polymer-mediated B cell TLR7/8 activation, and (v.) the resulting T cell help required for robust, durable antibody responses. (**b**) Synthesis of p(TLR-*b*-Fent) by reversible addition-fragmentation chain-transfer (RAFT) polymerization. The first block, p(TLR), was synthesized by copolymerizing the TLR7/8 agonist monomer mTLR (2) with the biologically inert comonomer mGlyc (3) using a bifunctional fentanyl- and azide-terminated RAFT agent (1). The polymer was subsequently chain-extended *in situ* with mFent (5) and mGlyc (3) to generate p(TLR-*b*-Fent). (**c**) Schematic of the final polymeric fentanyl vaccine (pTFV), prepared by copper-free click conjugation of azide-terminated p(TLR-*b*-Fent) to DBCO-functionalized CRM_{197} containing a PEGylated self-immolative linker, and the mechanism of intracellular linker degradation and carrier protein release. (**d**) SEC-HPLC chromatograms of CRM_{197}, CRM_{197}-DBCO, and pTFV, where left shift indicates increasing molecular weight. (**e**) Experimental design evaluating the importance of molecular integration of vaccine components. C57BL/6J mice (n = 6/group) were vaccinated (s.c.) on day 0 with saline, pTFV, pFV + mTLR, or CRM_{197} + p(TLR-*b*-Fent). Vaccine formulations contained 10 µg CRM_{197} and 10 µg mTLR, where applicable. (**f**) Serum anti-fentanyl IgG titers at week 9. (**g**) Antibody avidity index, defined as the guanidine hydrochloride concentration required to reduce normalized absorbance by 50% (ID_{50}). (**h**) Percent maximum possible effect (%MPE) at week 9. (**i**) Experimental design comparing block and random polymer architectures. C57BL/6J mice (n = 6/group) were vaccinated (s.c.) on days 0 and 21 with saline, pTFV, or pTFV-R at doses containing 10 µg CRM_{197} and 10 µg mTLR. Serum anti-fentanyl IgG responses were evaluated for 7 weeks. (**j**) Serum anti-fentanyl IgG titers at weeks 2, 5, and 7. (**k**) Antibody avidity index (ID_{50}). (**l**) %MPE determined by hot-plate assay following fentanyl challenge (0.3 mg/kg, i.p.) at week 7. Statistical differences in (**f, g, h,** and **l**) were evaluated by ordinary one-way ANOVA with Tukey's multiple comparisons test and unpaired t-test as Mann-Whitney test with compared ranks between each group in **j** and **k**. Horizontal lines identify the groups being compared, and P values are shown above the corresponding lines. Data are presented as mean ± SD, with individual points representing individual mice.

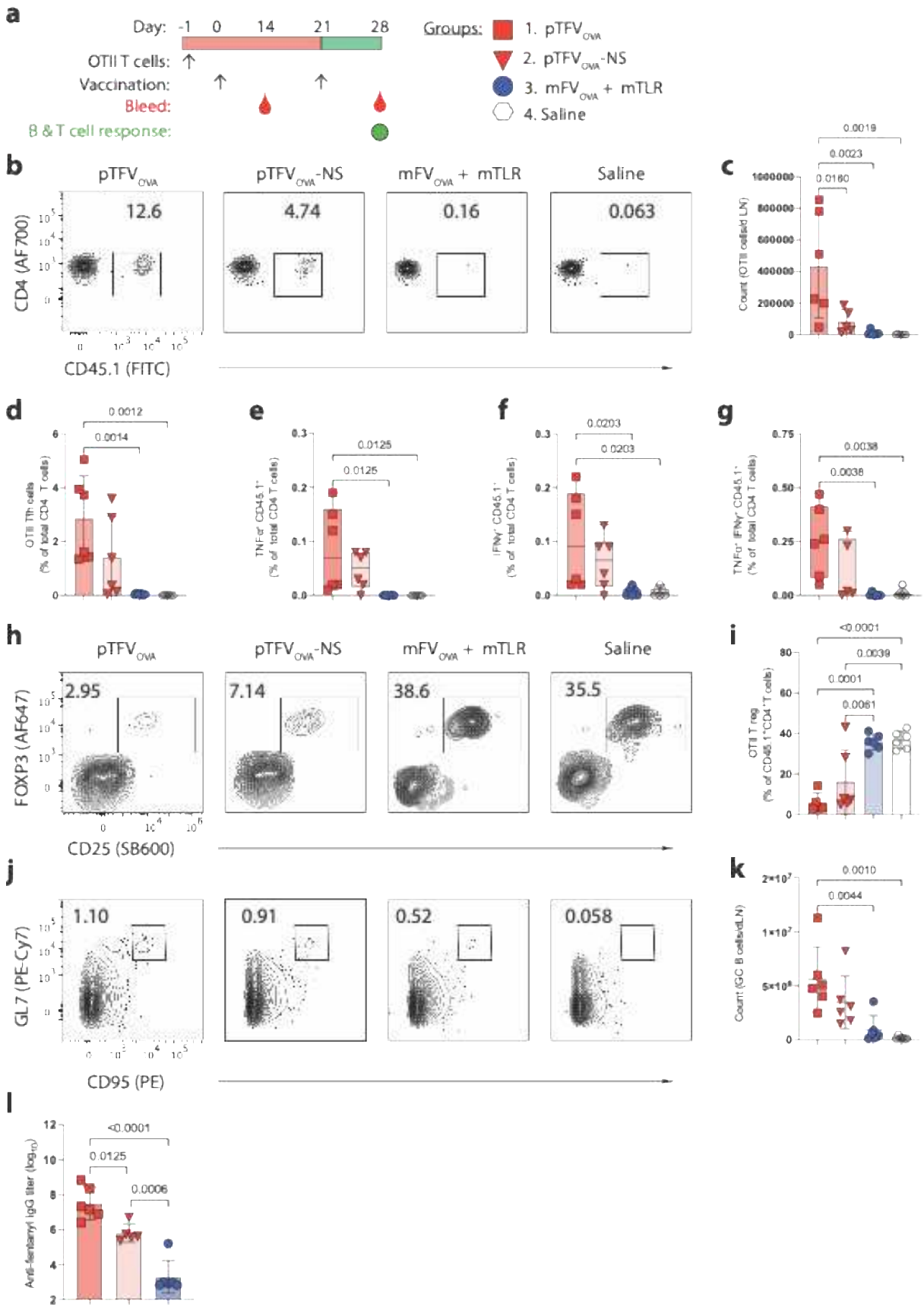
a
Day: -1 0 14 21 28
OTII T cells:
Vaccination:
Bleed:
B & T cell response:
Groups:
1. pTFV$_{OVA}$
2. pTFV$_{OVA}$-NS
3. mFV$_{OVA}$ + mTLR
4. Saline
b
pTFV$_{OVA}$
pTFV$_{OVA}$-NS
mFV$_{OVA}$ + mTLR
Saline
12.6
4.74
0.16
0.063
CD4 (AF700)
CD45.1 (FITC)
c
0.0019
0.0023
0.0160
Count (OTII cells/sd LN)
d
0.0012
0.0014
OTII Th cells (% of total CD4 T cells)
e
0.0125
0.0125
TNFα+ CD45.1+ (% of total CD4 T cells)
f
0.0203
0.0203
IFNγ+ CD45.1+ (% of total CD4 T cells)
g
0.0038
0.0038
TNFα+ IFNγ+ CD45.1+ (% of total CD4 T cells)
h
pTFV$_{OVA}$
pTFV$_{OVA}$-NS
mFV$_{OVA}$ + mTLR
Saline
2.95
7.14
38.6
35.5
FOXP3 (AF647)
CD25 (SB600)
i
<0.0001
0.0039
0.0001
0.0061
OTII T reg (% of CD45.1+CD4+ T cells)
j
1.10
0.91
0.52
0.058
GL7 (PE-Cy7)
CD95 (PE)
k
0.0010
0.0044
Count (GC B cells/dLN)
l
<0.0001
0.0125
0.0006
Anti-fentanyl IgG titer (log$_{10}$)

Figure 2. Self-immolative carrier release enhances carrier-specific T-cell help and germinal-center responses. (**a**) To monitor CP-specific T cell responses, C57BL/6J mice (n = 6/group) received an adoptive transfer of 7.5 x 10^5 OVA-specific OTII T cells per mouse one day before prime immunization. Mice were vaccinated (s.c.) on days 0 and 21 with saline, or 18 μg of $pTFV_{OVA}$, $pTFV_{OVA}$-NS, or mFV_{OVA} + mTLR. On day 28, the OVA-specific T cell and GC B cell responses in the dLN and serum antibody response were measured via flow cytometry and ELISA, respectively. (**b**) Representative flow cytometry gating identifying OTII T cells ($CD3^+CD4^+CD45.1^+$) as a percentage of $CD4^+$ T cells and (**c**) total number of OTII T cells in the dLN on day 28. (**d**) Percent Fraction of OTII Tfh cells ($CD3^+CD4^+CD45.1^+CD44^+CXCR5^+Bcl\text{-}6^{hi}$) in the dLN. (**e-g**) Percent fraction of (**e**) $TNF\alpha^+$, (**f**) $IFN\gamma^+$, and (**g**) multifunctional $IFN\gamma^+TNF\alpha^+$ $CD4^+$ T cells in dLN cell populations upon *ex vivo* antigen restimulation. (**h**) Representative flow cytometry gating identifying OTII Tregs ($CD3^+CD4^+CD45.1^+CD25^+FOXP3^+$) and (**i**) fraction of OTII Tregs in the dLN on day 28. (**j**) Representative flow cytometry gating identifying GC B cells ($CD19^+B220^+GL7^+CD95^+$) and (**k**) number of GC B cells in the dLN. (**l**) Anti-fentanyl antibody titers on day 28. Statistical comparisons evaluated by ordinary one-way ANOVA with Tukey's multiple comparisons test. Statistical comparisons are indicated by horizontal bars with superscript *P* values. Data presented as mean ± SD, with individual points representing individual mice. Data are representative of two independent experiments that produced similar results.

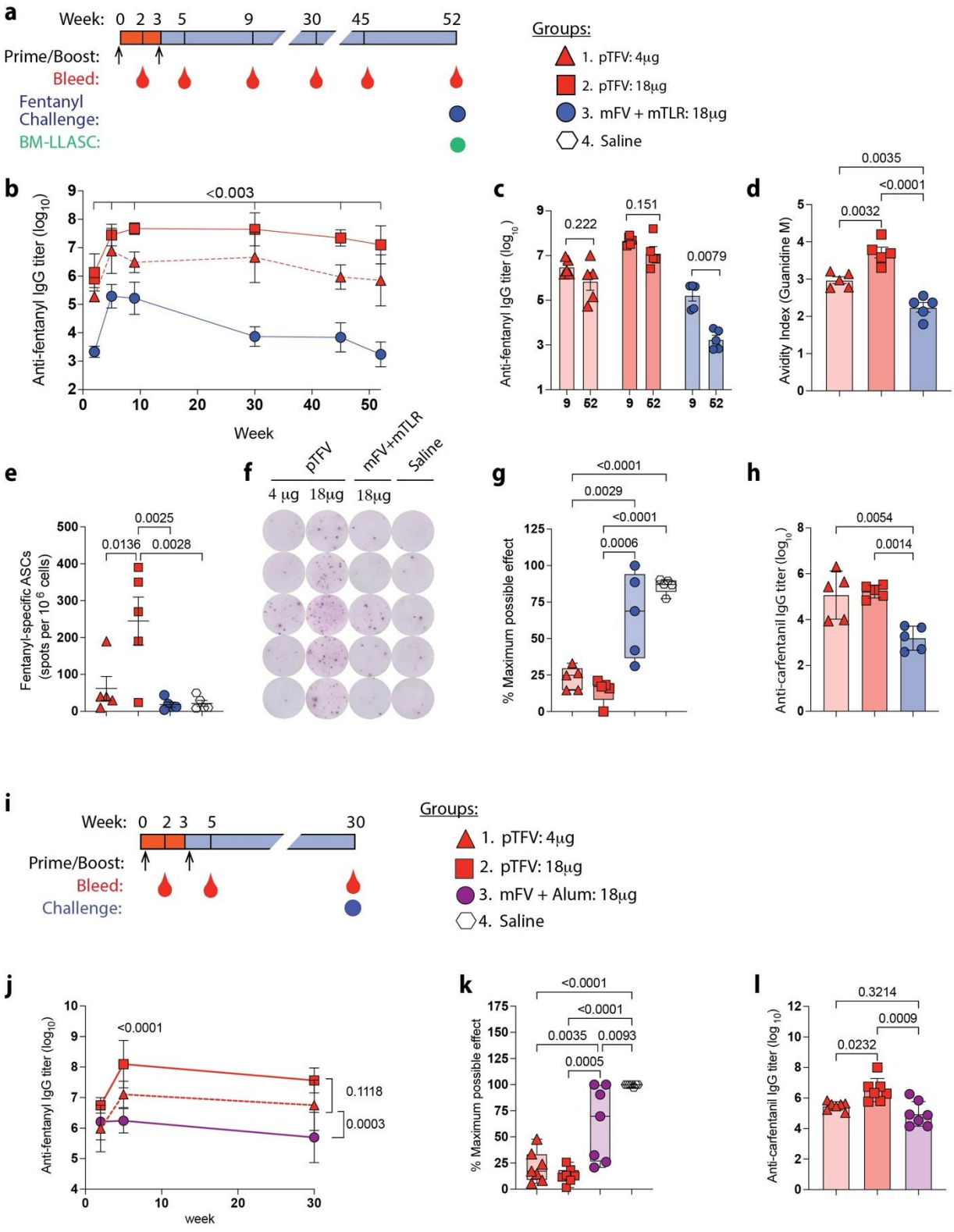

Figure 3: pTFV provides durable protection at lower doses than monomeric fentanyl vaccine. (**a**) C57BL/6J Mice (n = 5/group) were vaccinated (s.c.) on days 0 and 21 with saline,

pTFV (4 or 18 μg), or mFV + mTLR (18 μg). Serum anti-fentanyl IgG responses were evaluated longitudinally for 52 weeks, followed by fentanyl challenge and analysis of bone marrow LLASCs at week 52. (**b**) Anti-fentanyl IgG titers over 52 weeks. (**c**) Anti-fentanyl IgG titer response comparison at week 9 (peak) and week 52 (late). (**d**) Avidity index presented as the guanidine hydrochloride concentration required to reduce normalized absorbance by 50% (ID50). (**e-f**) Relative number (**e**) of anti-fentanyl-specific ASCs in the bone marrow and (**f**) representative images of B cell ELISpots at week 52. (**g**) Percent maximum possible effect determined via hot plate assay after fentanyl challenge (0.3mg/kg, i.p) at week 52. (**h**) Anti-carfentanil IgG titer at week 52. (**i**) C57BL/6J Mice (n = 6/group) were vaccinated (s.c.) on day 0 and 21 with saline, pTFV (4 or 18 μg), or mFV + Alum (18 μg of equiv. aluminum). (**j**) Anti-fentanyl IgG titers over 30 weeks. (**k**) Percent maximum possible effect determined via hot plate assay upon fentanyl challenge (0.3mg/kg, i.p.) at week 30. (**l**) Anti-carfentanil IgG titer at week 30. Statistical comparison in (**c**) made with unpaired t-test as Mann-Whitney test with compared ranks between each group at week 9 and week 52. All other statistical differences evaluated by ordinary one-way ANOVA with Tukey's multiple comparisons test. In (**b**), horizontal bars and superscript *P* values indicate statistical differences between pTFV and mFV + mTLR. All other comparisons are indicated by horizontal bars with superscript *P* values. Data are presented as mean ± SD, with individual points representing individual mice. Data are representative of two independent experiments that produced similar results.

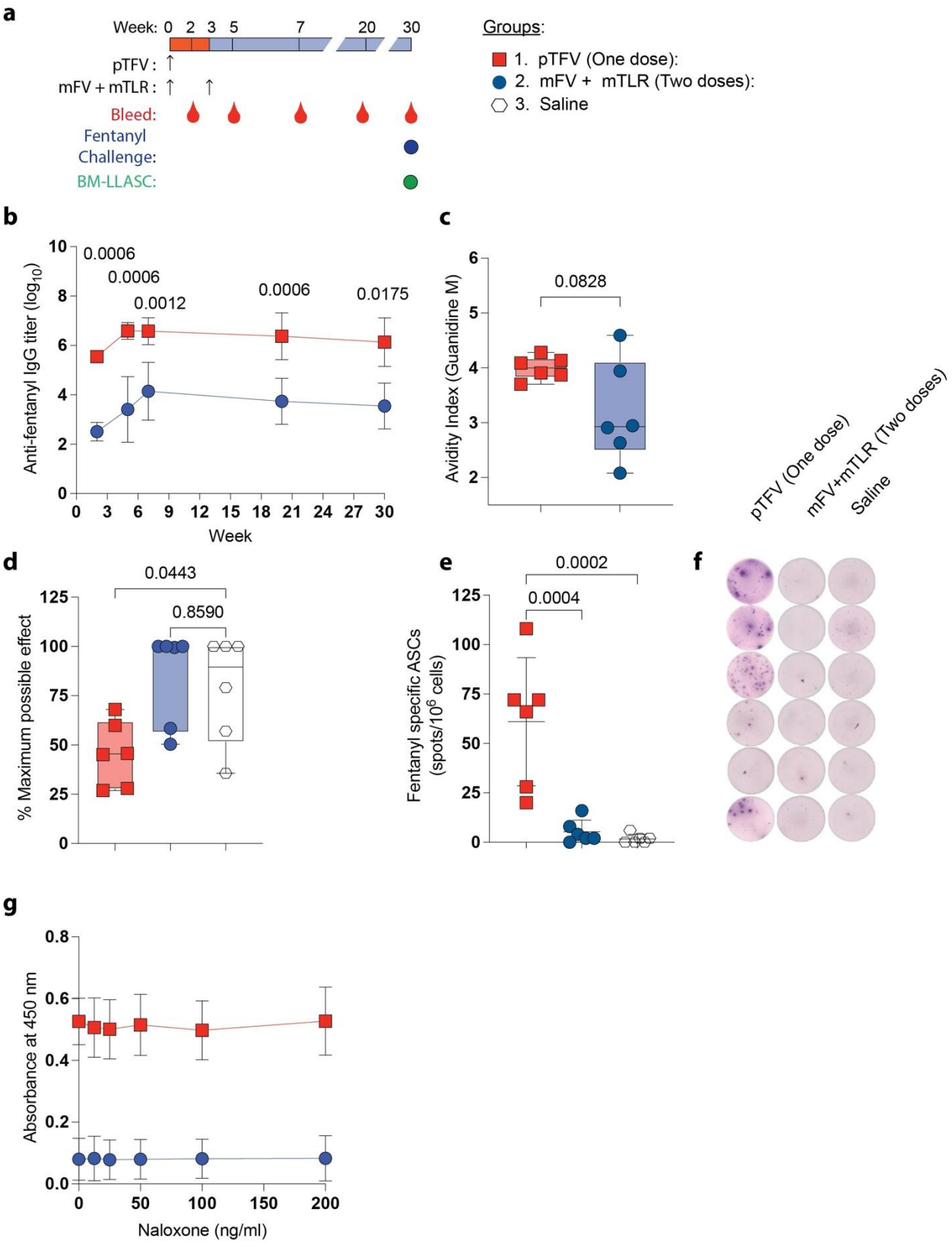

Figure 4: A single dose of pTFV elicits a more robust, protective immune response than

two doses of monomeric vaccine. (**a**) C57BL/6J Mice (n = 6/group) were vaccinated (s.c.) once with pTFV (4 μg) on day 0 or twice with mFV + mTLR (4 μg/dose) or saline on days 0 and 21. Serum anti-fentanyl IgG responses were evaluated longitudinally for 30 weeks, followed by fentanyl challenge and analysis of bone marrow LLASCs at week 30. (**b**) Anti-fentanyl IgG titers over 30 weeks. (**c**) Avidity index presented as the guanidine hydrochloride concentration required to reduce normalized absorbance by 50% (ID50). (**d**) Percent maximum possible effect determined via hot plate assay after fentanyl challenge (0.3mg/kg, i.p) at week 30. (**e**) Relative numbers of fentanyl-specific LLASCs in the bone marrow and (**f**) representative ELISpot images at week 30. (**g**). Absorbance at 450 nm vs. naloxone concentration (ng/mL) for competitive inhibition ELISA. Statistical comparisons in (**b**) and (**c**) made by unpaired t-test as Mann-Whitney test with compared ranks at week 2, 5, 7, 20 and 30 between single-dose pTFV and two-dose mFV + mTLR. Statistical differences in (**d**) and (**e**) were evaluated by ordinary one-way ANOVA with Tukey's multiple-comparisons test and are indicated by *P* values. All other comparisons are indicated by horizontal bars with superscript *P* values. Data are presented as mean ± SD, with individual points representing individual mice. Data are representative of two independent experiments that produced similar results.

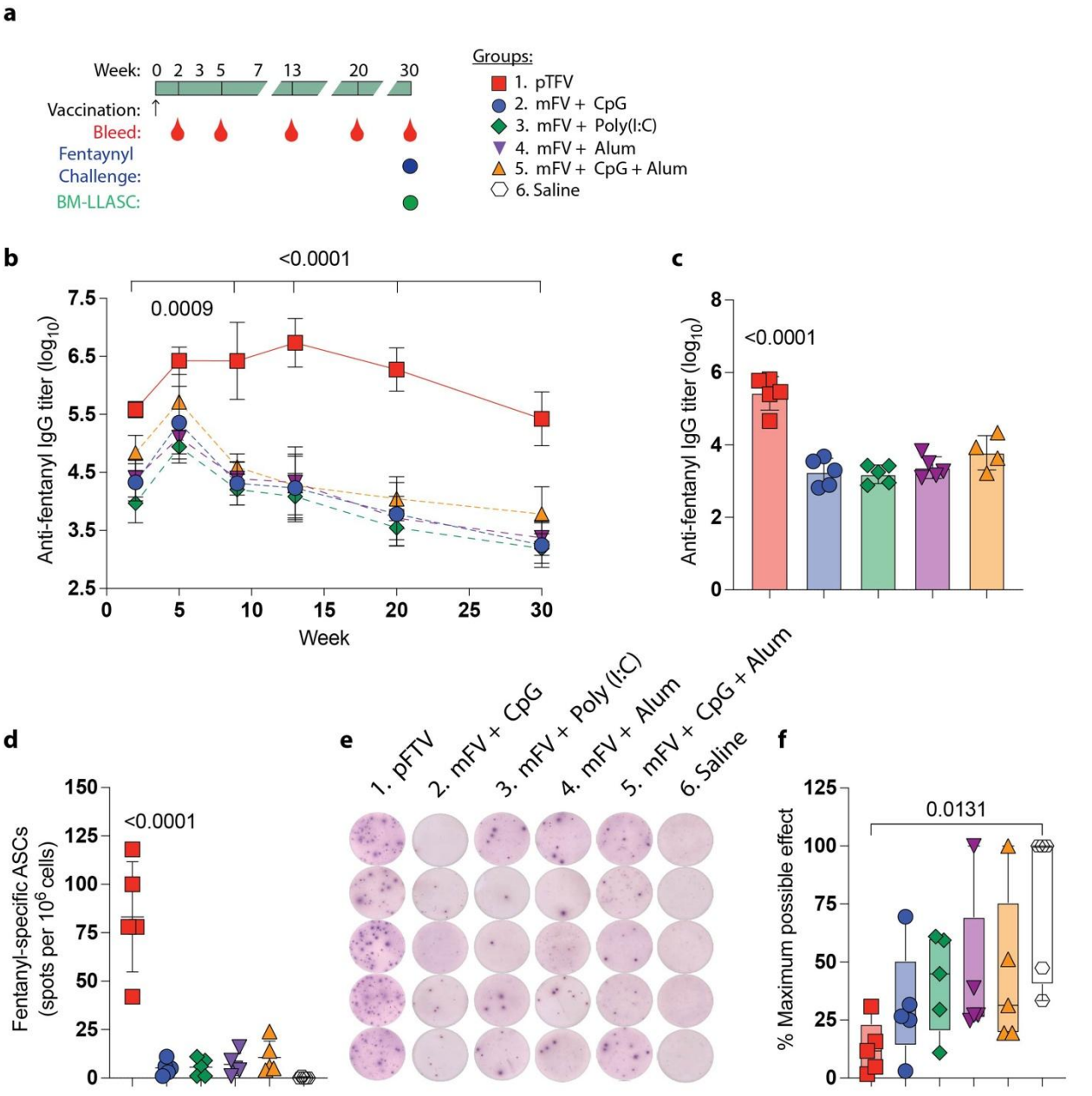

Figure 5. Integrated polymer vaccine architecture provides superior single-dose protection compared with conventional adjuvant formulations. (**a**) On day 0, C57BL/6J mice (n = 6/group) were vaccinated (s.c.) with saline, pTFV (10 µg of mTLR), or mFV admixed with 10 µg of CpG, or poly (I:C), or alum, or mFV admixed with 5µg each of CpG + alum. Serum anti-fentanyl IgG responses were evaluated longitudinally for 30 weeks, followed by fentanyl challenge and analysis of bone marrow LLASCs at week 30. (**b**) Anti-fentanyl IgG titers over 30 weeks. (**c**) Week 30 anti-fentanyl IgG titers. (**d-e**) Relative number (**d**) of fentanyl-specific LLASCs in the bone marrow and (**e**) representative B cell ELISpot images at week 30. (**f**) Percent maximum

possible effect determined via hot plate assay after fentanyl challenge (0.3mg/kg, i.p) at week 30. Statistical differences were evaluated by ordinary one-way ANOVA with Tukey's multiple-comparisons test comparing pTFV with all other groups and are indicated by *P* values. Data presented as mean ± SD, with individual points representing individual mice. Data are representative of two independent experiments that produce similar results.

Supplementary Files

This is a list of supplementary files associated with this preprint. Click to download.

- SupplementaryinformationKumaretal.docx